Nanoscale Research Letters
a SpringerOpen Journal

NANO EXPRESS Open Access

Statistical characteristics of reset switching in $Cu/HfO_2/Pt$ resistive switching memory

Meiyun Zhang[1], Shibing Long[1*], Guoming Wang[1], Ruoyu Liu[1], Xiaoxin Xu[1], Yang Li[1], Dinlin Xu[1], Qi Liu[1], Hangbing Lv[1], Enrique Miranda[2], Jordi Suñé[2] and Ming Liu[1]

Abstract

A major challenge of resistive switching memory (resistive random access memory (RRAM)) for future application is how to reduce the fluctuation of the resistive switching parameters. In this letter, with a statistical methodology, we have systematically analyzed the reset statistics of the conductive bridge random access memory (CBRAM) with a $Cu/HfO_2/Pt$ structure which displays bipolar switching property. The experimental observations show that the distributions of the reset voltage (V_{reset}) and reset current (I_{reset}) are greatly influenced by the initial on-state resistance (R_{on}) which is closely related to the size of the conductive filament (CF) before the reset process. The reset voltage increases and the current decreases with the on-state resistance, respectively, according to the scatter plots of the experimental data. Using resistance screening method, the statistical data of the reset voltage and current are decomposed into several ranges and the distributions of them in each range are analyzed by the Weibull model. Both the Weibull slopes of the reset voltage and current are demonstrated to be independent of the on-state resistance which indicates that no CF dissolution occurs before the reset point. The scale factor of the reset voltage increases with on-state resistance while that of the reset current decreases with it. These behaviors are fully in consistency with the thermal dissolution model, which gives an insight on the physical mechanism of the reset switching. Our work has provided an inspiration on effectively reducing the variation of the switching parameters of RRAM devices.

Keywords: RRAM; Statistics; Conductive filament; Weibull model; Thermal dissolution

Background

Resistive random access memory (RRAM), making full use of the reversible resistive switching (RS) effect of transition metal oxide to realize information storage, has been considered as a promising technology for high-density nonvolatile memory [1-4]. Due to its easy fabrication, promising performances, and feasibility of 3-D arrays, RRAM device, with a simple metal-insulator-metal (MIM) structure, has attracted considerable attention recently [5,6]. A majority of works have focused on exploring the underlying switching mechanism for most transition metal oxide materials in set and reset processes [7-11]. Generally, the formation and rupture of a tiny conductive filament (CF) in the metal oxides is proposed to explain the resistive switching phenomena between a high-resistance state (HRS) or off-state and a low-resistance state (LRS) or on-state. Oxygen vacancies as well as metal ions are widely accepted as playing a dominant role in the formation and disruption of filament under the influence of external stress [12]. However, the size and location of CF in the set process and the extent of the CF dissolution during the reset process display random behaviors in RRAM devices, which causes the formation and rupture of the CF intrinsically stochastic [13] and results in the variation of the switching parameters and negatively affects the commercial application of RRAM [14-17]. Thus, studying the statistical characteristics of the switching parameters and deepening the understanding of the underlying physical mechanism behind the RS statistics are beneficial to the effective control and trustful forecast of the memory performance and reliability [18-23].

In this letter, we have investigated the reset statistical characteristics of the conductive bridge random access memory (CBRAM) device based on a $Cu/HfO_2/Pt$

* Correspondence: longshibing@ime.ac.cn
[1]Lab of Nanofabrication and Novel Device Integration, Institute of Microelectronics, Chinese Academy of Sciences, Beijing 100029, China
Full list of author information is available at the end of the article

structure connected to a transistor. The experimental results show that the reset voltage increases with on-state resistance and the reset current decreases with it, which can be well explained by the thermal dissolution model. Since the on-state resistance has strong influence on the reset switching parameters, the resistance screening method is employed to decompose the resistance into several ranges. The distributions of the reset voltage and current studied in different resistance ranges are compatible with the Weibull model. The Weibull slopes of reset voltage and current have nothing to do with the on-state resistance. The scale factor of the reset voltage linearly increases with the on-state resistance while that of the reset current decreases with it in linearity, respectively. These results are all consistent with the thermal dissolution model. Our work is of great significance on the deep understanding of the switching mechanism and the improvement of the uniformity of RRAM devices.

Methods

Figure 1a shows the fabricated 1T1R (one transistor and one RRAM cell) structure with which the RS statistics of the Cu/HfO_2/Pt RRAM device are investigated. N^+ type transistor was made up by standard 0.13 μm CMOS process of SMIC. Cu plug connected to the drain of the transistor was flattened by the chemical mechanical polished (CMP) and is used as the bottom electrode (BE) of our RRAM cell. A HfO_2 RS layer was deposited by ion beam sputtering with a thickness of 6 nm on the Cu plug. Pt top electrode (TE) was then prepared by e-beam evaporation and patterned by lift-off process. The transistor in the 1T1R structure is used as the current compliance in the forming and set operation for RRAM cell to prevent the hard dielectric breakdown of the HfO_2 layer and the overshoot of the current [24]. The electrical characteristics of the device were measured by Agilent B1500A Semiconductor Device Parameter Analyzer (Agilent Technologies, Inc., Santa Clara, CA, USA). The *I-V* curves in the 4,000 continuous set/reset cycles for the RRAM cell are tested under the DC voltage sweep mode. During the measurement, the voltage sweeping was applied on the source terminal in the set operation and on the drain terminal during the reset process, with the value of the voltage ramped from 0 to 2 V. The gate bias voltage of the transistor was set up as 2.5 V for the set operation to maintain a source-drain current of 1 mA to acquire an excellent current compliance and to avoid the RRAM cell being damaged by the current overshoot. In the reset operation, the gate bias was 3.3 V to guarantee that the CF is completely ruptured.

Results and discussion

Figure 1b presents several *I-V* curves of the Cu/HfO_2/Pt RRAM device. The metal-CF-type Cu/HfO_2/Pt devices

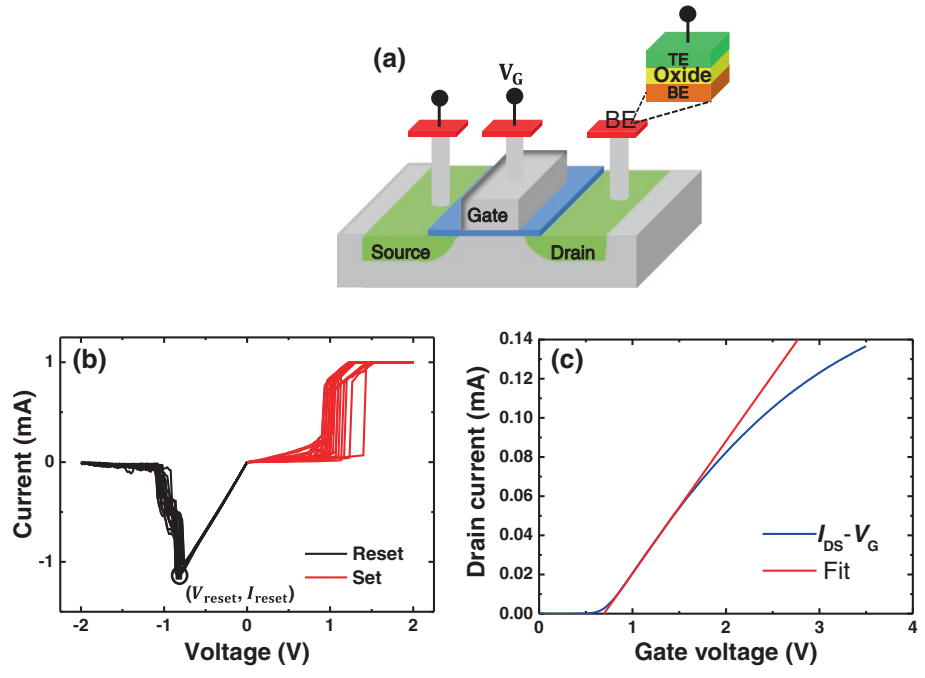

Figure 1 Characteristics of the RRAM device and the transistor. (a) The schematic of 1T1R structure. **(b)** Typical *I-V* curves of the Cu/HfO_2/Pt device in set and reset cycles. The reset points have been notated by V_{reset} and I_{reset}. **(c)** The transfer curve of the N^+ transistor. The intrinsic parameters of the transistor (including $Wu_nC_{ox}/2L$ and V_T) are abstracted from the slope and the intercept of the fitting line, so the soure-drain resistance is obtained from calculation.

are operated in a bipolar mode. The point with the maximum value of current is defined as the reset point at which the voltage and current are recorded as the V_{reset} and I_{reset}. We find that after the reset point, a series of current jumps occur during the reset process and the device finally switches to HRS. Through linear fitting to the reset *I-V* curve at the low-voltage region before the reset point, the on-state resistance of the 1T1R structure (R_{on_total}) is obtained, which is a sum of the LRS resistance of RRAM cell (R_{on}) and the source-drain resistance of the transistor (R_{DS}). R_{on} is then got through correcting R_{on_total} by R_{DS}. R_{DS} is usually in the order of several hundreds of ohms, which is comparable to R_{on}, so it should not be neglected during the reset process of RRAM device in 1T1R structure. Figure 1c shows a tested transfer characteristic curve ($I_{DS} - V_G$ curve) of the transistor with the source-drain voltage fixed to be 0.05 V. Through fitting the curve according to the output characteristic of the transistor with the equation $I_{DS} = \frac{Wu_nC_{ox}}{2L}\left[2(V_G - V_T)V_{DS} - V_{DS}^2\right]$, the intrinsic values of $Wu_nC_{ox}/2L$ and V_T are obtained, where u_n is the electronic mobility, W is the gate width, L is the gate length, and C_{ox} is the capacitance of the gate oxide. Based on the output characteristic curve ($I_{DS} - V_{DS}$ curve) of the transistor in the reset operation under $V_G = 3.3$ V, the source-drain resistance is available to be 300 Ω in average according to $R_{DS} = V_{DS}/I_{DS}$. Here, I_{DS} is the measured current flowing through the transistor and the RRAM device, and V_{DS} is calculated from the above equation using the abstracted $Wu_nC_{ox}/2L$ and V_T value and the measured I_{DS} values.

The relationships of V_{reset} and I_{reset} with R_{on} are studied with a statistical method. Figure 2a,b shows the scatter plots of V_{reset} and I_{reset} as a function of R_{on} in the 4,000 continuous set and reset cycles. As can be seen, the spread of V_{reset} and I_{reset} is slightly wide and V_{reset} increases while I_{reset} decreases with R_{on}. These characteristics can be accounted for by the thermal dissolution model [21-23,25-28] which assumes that reset is determined by the diffusion of the conductive defects. In Cu/HfO_2/Pt RRAM device, the conductive defects are mainly the Cu metal atoms or ions. When the local CF temperature reaches a critical value T_{reset}, the conductive defects begin to diffuse out of the CF and then reset occurs. Considering the balance between Joule dissipation and heat evacuation, the local temperature of the CF can be calculated by the basic equation $T_{reset} = T_0 + (R_{TH}/R_{on})V_{reset}^2$, where T_0 is the operation temperature, V_{reset} is the voltage dropped on the CF at the reset point, and R_{TH} is the thermal resistance describing heat dissipation from the CF to the environment. The thermal resistance R_{TH} can be divided into two components in parallel, the parallel

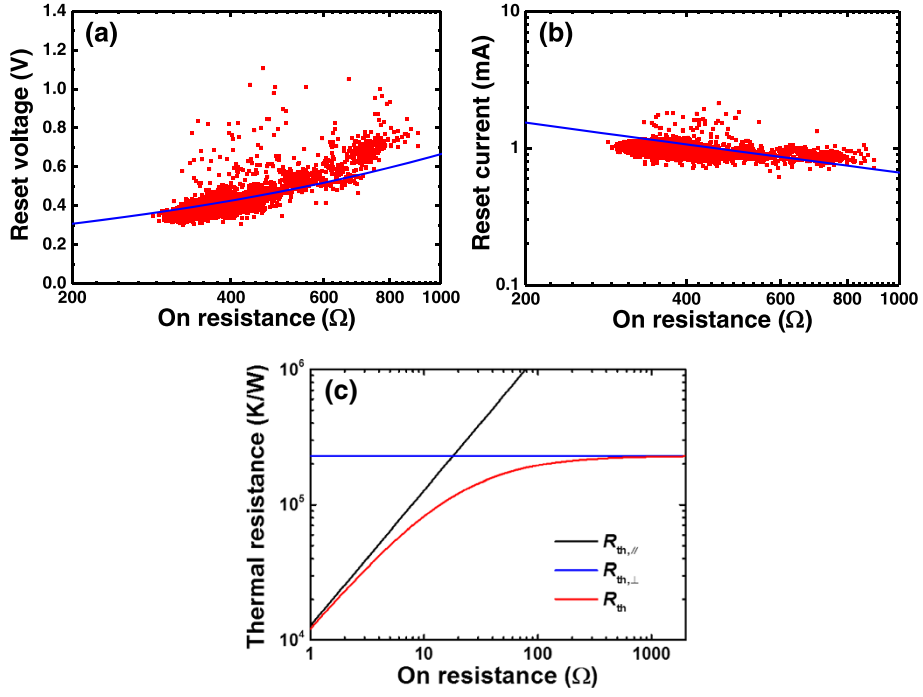

Figure 2 Scatter plots of V_{reset} and I_{reset} and dependence of the calculated R_{TH} on R_{on}. The dependence of the V_{reset} **(a)** and I_{reset} **(b)** as a function of R_{on}. V_{reset} increases and I_{reset} decreases with R_{on}, respectively, which are well fitted by the thermal dissolution model (blue lines) with $T_{reset} = 400$ K, $R_{TH,\perp} = 2.3 \times 10^5$ K/W. **(c)** The dependence of calculated thermal resistance on the CF resistance. $R_{TH,\perp}$ is considered as being constant with a value of 2.3×10^5 K/W.

resistance ($R_{TH,\parallel}$) and the perpendicular resistance ($R_{TH,\perp}$). Their relation is described by $R_{TH} = R_{TH,\parallel}R_{TH,\perp}/(R_{TH,\parallel} + R_{TH,\perp})$, where $R_{TH,\parallel} = R_{on}/(8LT_{reset})$ according to the Wiedemann-Franz (WF) law and $L = 2.45 \times 10^{-8}$ WΩK^{-2} is the Lorentz number [23]. The two components respectively describe the heat diffusion along the CF and from the CF surface to the surrounding oxide. Figure 2c shows the dependence of the calculated R_{TH} on R_{on}. At the low-resistance region, the value of R_{TH}/R_{on} is roughly constant and then when R_{on} increases, the ratio will not be constant anymore. Using the above relations, we can get the theoretical fittings for the experimental relationships between V_{reset}, I_{reset}, and R_{on} through choosing appropriate parameters of T_{reset} and $R_{TH,\perp}$. By the theoretical fitting, V_{reset} is proved to increase with R_{on}, which is consistent with our experimental results shown in Figure 2a. In this work, the on-state resistance is comparatively high, as compared with the reports in [21,22], so V_{reset} increases with R_{on}. This increase trend is similar to the $V_{reset2} - R_{reset2}$ relation reported in [23]. Since the CF behaves like a metallic conductor before the reset point [29], I_{reset} is inversely proportional to R_{on} as presented in Figure 2b.

To further study the details of the relationship of V_{reset} and I_{reset} as a function of R_{on}, the resistance screening method is utilized through which R_{on} is reasonably divided into several ranges. The statistical distributions of V_{reset} and I_{reset} in different ranges decomposed by the resistance method are studied in detail. Figure 3a shows the experimental distributions of V_{reset} in different R_{on} ranges in the Weibull plot. Figure 3b shows the typical distributions of V_{reset} in three different resistance ranges with linear fitting lines. We can conclude that the Weibull distribution can be used to well describe the experimental distributions of V_{reset} and I_{reset} of the Cu/HfO_2/Pt device. In Figure 3a,b, we find a high-percentile tail exists in the distribution in each R_{on} range, which is deviated from the standard Weibull distribution which is a straight line in the Weibull plot. Figure 3c shows the same three distributions in Figure 3b in the Gumbel plot, which can show more clearly the high-percentile tail region in the Weibull plot. As shown in Figure 3c, it can be seen that the experimental data in the high-percentile tail region in Figure 3b are just a very small part in the whole distribution in each range. Fitting all the experimental results in Figure 3a by linear Weibull distribution, the shape factors (i.e., the Weibull slopes) and the scale factors of V_{reset} distributions can be obtained. Figure 3d shows the dependence of the shape factor (β_V) and scale factor ($V_{63\ \%}$) of V_{reset} distributions on R_{on}. We can find that the Weibull slope of V_{reset} distribution remains constant and the scale factor of the V_{reset} distributions increases with R_{on}.

Analogous to the study of the reset voltage, the reset current are analyzed in the same way. Figure 4a,b shows the Weibull distributions of I_{reset} in different R_{on} ranges

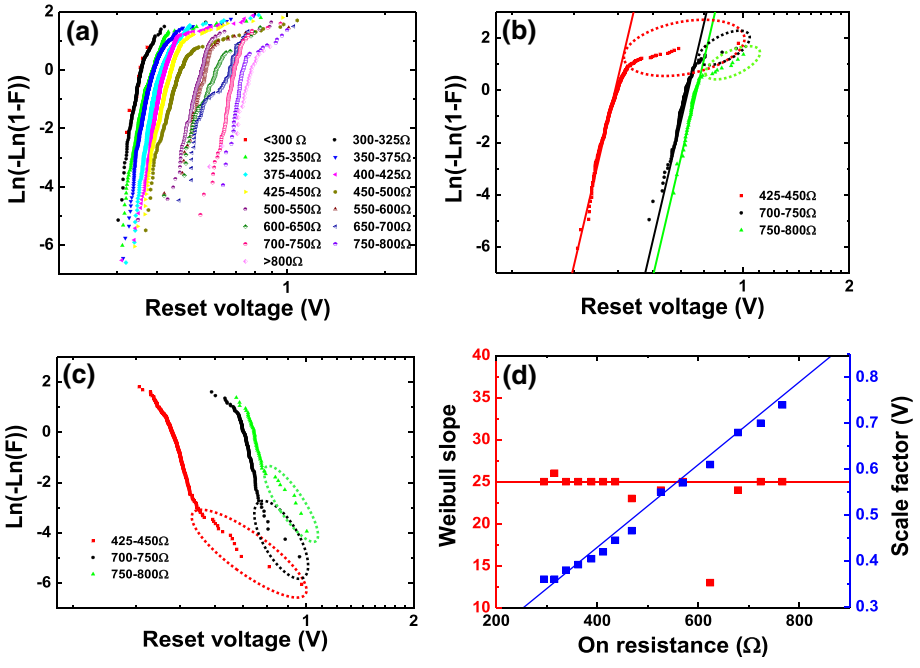

Figure 3 Experimental distributions of V_{reset} as a function of R_{on}. **(a)** Experimental distributions of V_{reset} in different R_{on} ranges in Weibull plot. **(b)** Distributions of V_{reset} with fitting lines in three resistance ranges. The fitting lines show that the experimental distributions are roughly compatible with Weibull distributions. **(c)** The Gumbel distribution of V_{reset} in the same three resistance ranges as in **(b)**. A small part of data fall into the circles, indicating that a small proportion of data belong to the tailing region of the distributions in **(b)**. **(d)** The dependence of the Weibull slope and scale factor of V_{reset} distribution on R_{on}. The Weibull slope remains constant and the scale factor increases linearly with R_{on}.

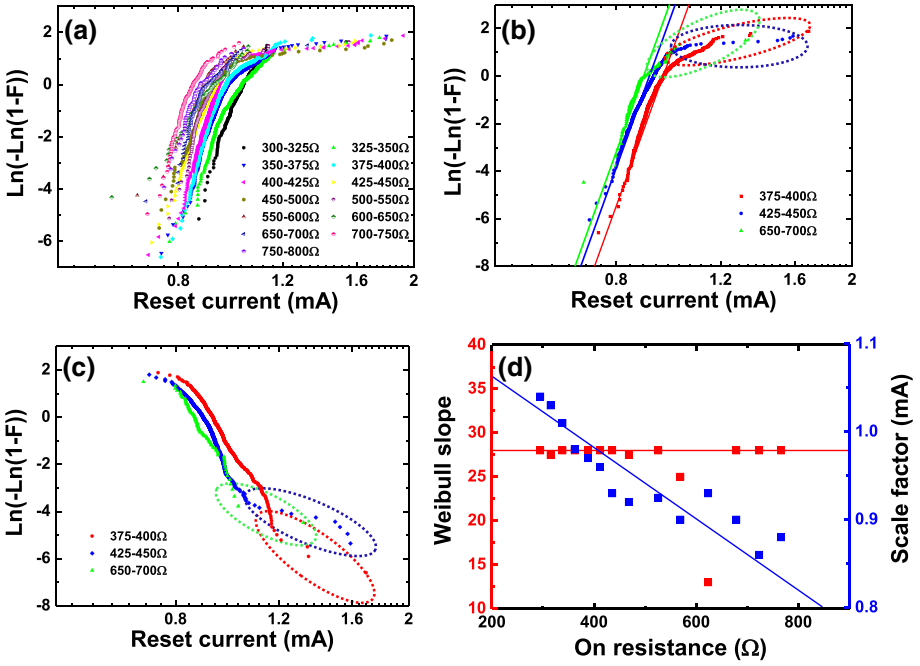

Figure 4 Experimental distributions of I_{reset} as a function of R_{on}. (a) Experimental distributions of I_{reset} in different R_{on} ranges in Weibull plot. **(b)** Distributions of I_{reset} with fitting lines in three R_{on} ranges. The fitting lines show that the experimental distributions are roughly compatible with Weibull distributions. **(c)** The Gumbel distribution of I_{reset} in the three R_{on} ranges same as those in **(b)**. A small part of data fall into the circles, indicating that a small proportion of data belong to the tailing region of the distributions in **(b)**. **(d)** The dependence of the Weibull slope and scale factor of I_{reset} distributions on R_{on}. The Weibull slope stays constant, and the scale factor decreases linearly with R_{on}.

with a certain high-percentile tails. These tails are also demonstrated to occupy only a small proportion by Gumbel distributions, as shown in Figure 4c. Through the linear fitting to the standard Weibull distributions, the abstracted Weibull slope and scale factor of the reset current distributions as a function of R_{on} are illustrated in Figure 4d. The Weibull slope of the reset current stays constant, and the scale factor decreases with R_{on}.

In our previous work [21], an analytical model based on the thermal dissolution model has been proposed for the unipolar reset statistics. Implementing this model into the experimental statistics of our Cu/HfO_2/Pt RRAM device, the abstracted Weibull slopes of V_{reset} and I_{reset} distributions, which are both independent on R_{on}, indicate that the reset point corresponds to the initial step of the CF dissolution in this device and there is no structural degradation before the reset point. This result can be evidenced by comparing the experimental and theoretical maximum CF temperature curves detailedly described in [22]. Figure 5 shows the experimental and theoretical reset temperature curves for two cycles of our Cu/HfO_2/Pt device. In Figure 5, before the reset point, the two types of curves are exactly in coincidence, which indicates that the reset point just corresponds to the starting point of the CF dissolution. In consequence, the statistical results of Cu/HfO_2/Pt RRAM device are compatible with the thermal dissolution model.

The above experiment and thermal dissolution model results both demonstrated that the statistical spread of reset parameters V_{reset} and I_{reset} are intrinsically limited by the on-state resistance R_{on}, so controlling the value and distribution of R_{on} is very critical to acquire high

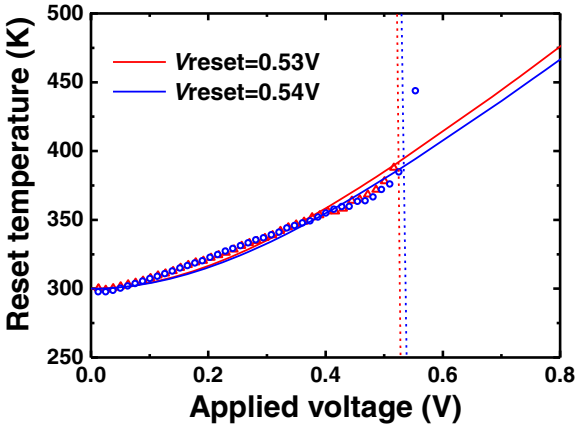

Figure 5 Experimental (symbols) and theoretical reset temperature (lines) of two reset cycles in the Cu/HfO_2/Pt device. The dashed lines indicate the reset voltage dropped on the RRAM cell, corresponding to the maximum current, i.e., the reset point. The experimental and theoretical curves nearly coincide before the reset point, so the reset point represents the starting point of the CF dissolution.

uniformity of reset switching. In the previous works, some methods have been proposed to reduce the variation of the off-state resistance (R_{off}) and on-state resistance (R_{on}), through which the uniformity of the set and reset switching parameters also have been improved and the set and reset events are controlled in certain ranges. These methods include: 1) doping impurities in the switching layer [30], selecting the electrode materials [31], and inserting interface layers [32] so as to effectively control the concentration and distribution of defects such as charge traps, metal ions, and oxygen vacancies etc.; 2) introducing the electric field-concentrating initiators (e.g., nanocrystals) on the bottom electrode to enhance the local electric field and reduce the random growth of filaments [16]; and 3) utilizing optimized operation methods [33]. In our recent work, we have also paid attention to the new pulse operation with regard to its role in improving the switching uniformity. Different from the traditional single pulse operation method in which only one wide pulse is applied in each switching cycle, a novel width/height-adjusting pulse operation method is proposed for RRAM. This method utilizes a series of pulses with the width or height increased gradually until a set or reset switching process is completely finished and no excessive stress is produced. The new operation method can exactly control the final resistance and significantly improve the uniformity, stability, and endurance of RRAM device. Additionally, we are also focusing on optimizing the device structure by etching the substrate into a cone shape on which the RRAM device is fabricated. The optimized structure can control the formation and rupture of the conductive filament in the oxide layer at the tip of the cone shape due to the high-generated electric field in this position. Thus, the variation of the switching parameters can be significantly reduced and the uniformity of these parameters will be improved.

Conclusions

In summary, we have studied the reset statistics of the CBRAM device with a Cu/HfO_2/Pt structure. The experimental results show that the reset voltage increases with on-state resistance and reset current decreases with it. The distributions of the reset voltage and current observed in different resistance ranges divided by 'resistance screening method' are compatible with the Weibull model. The Weibull slopes of reset voltage and current are constant, independent of the on-state resistance. The scale factors of the reset voltage increases and that of the reset current decreases with the on-state resistance in linearity, respectively. These results are in agreement with the thermal dissolution model. Our work is helpful in revealing the physics of the switching mechanism and giving guidelines to improve the uniformity of RRAM devices.

Competing interests
The authors declare that they have no competing interests.

Authors' contributions
MZ, GW, and SL did the statistical data analysis. SL, JS, and MZ interpreted the results. HL, SL, and ML designed the 1T1R samples. HL carried out the RRAM fabrication. RL and XX performed the electrical measurement. SL, JS, and ML participated in the design of the study and coordinated and supervised the whole work. ZM and SL drafted the manuscript. GW, YL, DX, QL, HL, EM, JS, and ML participated in the manuscript writing and discussion of results. All authors critically read and contributed to the manuscript preparation. All authors read and approved the final manuscript.

Acknowledgements
This work was supported by National Natural Science Foundation of China (NSFC) (Grant Nos. 61322408, 61221004, 61422407, 61334007, and 61274091), '973' Program (Grant No. 2011CBA00602) and '863' Program (Grant No. 2014AA032900) of Ministry of Science and Technology of China, Chinese Academy of Sciences Visiting Professorship for Senior International Scientists (Grant No. 2011T2G23), the Spanish Ministry of Science and Technology under contract TEC2012-32305 (partially funded by the FEDER program of the European Union), and the DURSI of the Generalitat de Catalunya under contract 2014SGR384. Jordi Suñé also acknowledges the ICREA Academia award.

Author details
[1]Lab of Nanofabrication and Novel Device Integration, Institute of Microelectronics, Chinese Academy of Sciences, Beijing 100029, China. [2]Departament d'Enginyeria Electrònica, Universitat Autònoma de Barcelona, Bellaterra 08193, Spain.

Received: 15 November 2014 Accepted: 11 December 2014
Published: 23 December 2014

References

1. Waser R, Dittmann R, Staikov G, Szot K: **Redox-based resistive switching memories-nanoionic mechanisms, prospects, and challenges.** *Adv Mater* 2009, **21:**2632–2663.
2. Yang JJ, Strukov DB, Stewart DR: **Memristive devices for computing.** *Nat Nanotechnol* 2013, **8:**13–24.
3. Waser R, Aono M: **Nanoionics-based resistive switching memories.** *Nat Mater* 2007, **6:**833–840.
4. Sawa A: **Resistive switching in transition metal oxides.** *Mater Today* 2008, **11:**28–36.
5. Pan F, Gao S, Chen C, Song C, Zeng F: **Recent progress in resistive random access memories: materials, switching mechanisms, and performance.** *Mater Sci Eng R* 2014, **83:**1–59.
6. Wong HSP, Lee HY, Yu S, Chen YS, Wu Y, Chen PS, Lee B, Chen FT, Tsai MJ: **Metal-oxide RRAM.** *Proc IEEE* 2012, **100:**1951–1970.
7. Yang Y, Gao P, Gaba S, Chang T, Pan X, Lu W: **Observation of conducting filament growth in nanoscale resistive memories.** *Nat Commun* 2012, **3:**732.
8. Peng S, Zhuge F, Chen X, Zhu X, Hu B, Pan L, Chen B, Li RW: **Mechanism for resistive switching in an oxide-based electrochemical metallization memory.** *Appl Phys Lett* 2012, **100:**072101.
9. Cagli C, Nardi F, Ielmini D: **Modeling of set/reset operations in NiO-based resistive switching memory devices.** *IEEE Trans Electron Devices* 2009, **56:**1712–1720.
10. Lu Y, Gao B, Fu Y, Chen B, Liu L, Liu X, Kang J: **A simplified model for resistive switching of oxide-based resistive random access memory devices.** *IEEE Electron Device Lett* 2012, **33:**306–308.
11. Ielmini D, Nardi F, Cagli C: **Physical models of size-dependent nanofilament formation and rupture in NiO resistive switching memories.** *Nanotechnology* 2011, **22:**254022.
12. Prakash A, Jana D, Maikap S: **TaO_X-based resistive switching memories: prospective and challenges.** *Nanoscale Res Lett* 2013, **8:**418.
13. Li Q, Khiat A, Salaoru I, Xu H, Prodromakis T: **Stochastic switching of TiO_2-based memristive devices with identical initial memory states.** *Nanoscale Res Lett* 2014, **9:**293.
14. Yu S, Guan X, Wong HSP: **On the switching parameter variation of metal-oxide RRAM-part II: model corroboration and device design strategy.** *IEEE Trans Electron Devices* 2012, **59:**1183–1188.

15. Guan X, Yu S, Wong HSP: **On the switching parameter variation of metal-oxide RRAM-part I: physical modeling and simulation methodology.** *IEEE Trans Electron Devices* 2012, **59:**1172–1182.
16. Liu Q, Long S, Lv H, Wang W, Niu J, Huo Z, Chen J, Liu M: **Controllable growth of nanoscale conductive filaments in solid-electrolyte-based ReRAM by using a metal nanocrystal covered bottom electrode.** *ACS Nano* 2010, **4:**6162–6168.
17. Lee S, Woo J, Lee D, Cha E, Hwang H: **Internal resistor of multi-functional tunnel barrier for selectivity and switching uniformity in resistive random access memory.** *Nanoscale Res Lett* 2014, **9:**364.
18. Luo WC, Liu JC, Lin YC, Lo CL, Huang JJ, Lin KL, Hou TH: **Statistical model and rapid prediction of RRAM SET speed-disturb dilemma.** *IEEE Trans Electron Devices* 2013, **60:**3760–3766.
19. Luo WC, Lin KL, Huang JJ, Lee CL, Hou TH: **Rapid prediction of RRAM RESET-state disturb by ramped voltage stress.** *IEEE Electron Device Lett* 2012, **33:**597–599.
20. Suñé J, Tous S, Wu EY: **Analytical cell-based model for the breakdown statistics of multilayer insulator stacks.** *IEEE Electron Device Lett* 2009, **30:**1359–1361.
21. Long S, Cagli C, Ielmini D, Liu M, Suñé J: **Reset statistics of NiO-based resistive switching memories.** *IEEE Electron Device Lett* 2011, **32:**1570–1572.
22. Long S, Lian X, Ye T, Cagli C, Perniola L, Miranda E, Liu M, Suñé J: **Cycle-to-cycle intrinsic RESET statistics in HfO_2-based unipolar RRAM devices.** *IEEE Electron Device Lett* 2013, **34:**623–625.
23. Long S, Perniola L, Cagli C, Buckley J, Lian X, Miranda E, Pan F, Liu M, Suñé J: **Voltage and power-controlled regimes in the progressive unipolar RESET transition of HfO_2-based RRAM.** *Sci Rep* 2013, **3:**2929.
24. Wan HJ, Zhou P, Ye L, Lin YY, Tang TA, Wu HM, Chi MH: **In situ observation of compliance-current overshoot and its effect on resistive switching.** *IEEE Electron Device Lett* 2010, **31:**246–248.
25. Russo U, Ielmini D, Cagli C, Lacaita AL: **Filament conduction and reset mechanism in NiO-based resistive-switching memory (RRAM) devices.** *IEEE Trans Electron Devices* 2009, **56:**186–192.
26. Russo U, Ielmini D, Cagli C, Lacaita AL: **Self-accelerated thermal dissolution model for reset programming in unipolar resistive-switching memory (RRAM) devices.** *IEEE Trans Electron Devices* 2009, **56:**193–200.
27. Russo U, Ielmini D, Cagli C, Lacaita AL, Spigat S, Wiemert C, Perego M, Fanciulli M: **Conductive-filament switching analysis and self-accelerated thermal dissolution model for reset in NiO-based RRAM.** *IEEE Int Electron Devices Meet Tech Dig* 2007, 775–778.
28. Zhou P, Ye L, Sun QQ, Wang PF, Jiang AQ, Ding SJ, Zhang DW: **Effect of concurrent joule heat and charge trapping on RESET for NbAlO fabricated by atomic layer deposition.** *Nanoscale Res Lett* 2013, **8:**91.
29. Wang M, Bi C, Li L, Long S, Liu Q, Lv H, Lu N, Sun P, Liu M: **Thermoelectric Seebeck effect in oxide-based resistive switching memory.** *Nat commun* 2014, **5:**4598.
30. Liu Q, Long S, Wang W, Zuo Q, Zhang S, Chen J, Liu M: **Improvement of resistive switching properties in ZrO_2-based ReRAM with implanted Ti ions.** *IEEE Electron Device Lett* 2009, **30:**1335–1337.
31. Wang Y, Liu Q, Long S, Wang W, Wang Q, Zhang M, Zhang S, Li Y, Zuo Q, Yang J, Liu M: **Investigation of resistive switching in Cu-doped HfO_2 thin film for multilevel non-volatile memory applications.** *Nanotechnology* 2010, **21:**045202.
32. Ryu SW, Ahn YB, Kim HJ, Nishi Y: **Ti-electrode effects of NiO based resistive switching memory with Ni insertion layer.** *Appl Phys Lett* 2012, **100:**133502.
33. Liu H, Lv H, Yang B, Xu X, Liu R, Liu Q, Long S, Liu M: **Uniformity improvement in 1T1R RRAM with gate voltage ramp programming.** *IEEE Electron Device Lett* 2014, **35:**1224–1226.

doi:10.1186/1556-276X-9-694
Cite this article as: Zhang *et al.*: Statistical characteristics of reset switching in Cu/HfO_2/Pt resistive switching memory. *Nanoscale Research Letters* 2014 **9**:694.